

## Video Article

# An *In Vivo* Blood-brain Barrier Permeability Assay in Mice Using Fluorescently Labeled Tracers

Kavi Devraj<sup>1,2</sup>, Sylvaine Guérit<sup>1</sup>, Jakranka Macas<sup>1</sup>, Yvonne Reiss<sup>1</sup><sup>1</sup>Institute of Neurology (Edinger Institute), Goethe University Hospital<sup>2</sup>Pharmazentrum Frankfurt, Institute for General Pharmacology and Toxicology, Goethe University HospitalCorrespondence to: Yvonne Reiss at [Yvonne.Reiss@kgu.de](mailto:Yvonne.Reiss@kgu.de)URL: <https://www.jove.com/video/57038>DOI: [doi:10.3791/57038](https://doi.org/10.3791/57038)Keywords: Neuroscience, Issue 132, Blood-brain barrier, BBB, *in vivo*, permeability, quantitative, fluorescent tracers, endothelial cells, microvessels, capillaries, intraperitoneal, perfusion

Date Published: 2/26/2018

Citation: Devraj, K., Guérit, S., Macas, J., Reiss, Y. An *In Vivo* Blood-brain Barrier Permeability Assay in Mice Using Fluorescently Labeled Tracers. *J. Vis. Exp.* (132), e57038, doi:10.3791/57038 (2018).

## Abstract

Blood-brain barrier (BBB) is a specialized barrier that protects the brain microenvironment from toxins and pathogens in the circulation and maintains brain homeostasis. The principal sites of the barrier are endothelial cells of the brain capillaries whose barrier function results from tight intercellular junctions and efflux transporters expressed on the plasma membrane. This function is regulated by pericytes and astrocytes that together form the neurovascular unit (NVU). Several neurological diseases such as stroke, Alzheimer's disease (AD), brain tumors are associated with an impaired BBB function. Assessment of the BBB permeability is therefore crucial in evaluating the severity of the neurological disease and the success of the treatment strategies employed.

We present here a simple yet robust permeability assay that have been successfully applied to several mouse models both, genetic and experimental. The method is highly quantitative and objective in comparison to the tracer fluorescence analysis by microscopy that is commonly applied. In this method, mice are injected intraperitoneally with a mix of aqueous inert fluorescent tracers followed by anesthetizing the mice. Cardiac perfusion of the animals is performed prior to harvesting brain, kidneys or other organs. Organs are homogenized and centrifuged followed by fluorescence measurement from the supernatant. Blood drawn from the cardiac puncture just before perfusion serves for normalization purpose to the vascular compartment. The tissue fluorescence is normalized to the wet weight and serum fluorescence to obtain a quantitative tracer permeability index. For additional confirmation, the contralateral hemi-brain preserved for immunohistochemistry can be utilized for tracer fluorescence visualization purposes.

## Video Link

The video component of this article can be found at <https://www.jove.com/video/57038/>

## Introduction

The blood-brain barrier (BBB) consists of the microvascular endothelial cells (ECs) supported by closely associated pericytes (PCs), which are ensheathed in the basal lamina, and astrocytes (ACs) that envelop the basement membrane with their end-feet<sup>1,2</sup>. ECs interact with several cell types that support and regulate the barrier function, primarily ACs and PCs, and also neurons and microglia, all of which together form the neurovascular unit (NVU). The NVU is critical for the function of the BBB, which limits the transport of blood-borne toxins and pathogens from entering the brain. This function is a result of tight-junction molecules such as claudin-5, occludin, zonula occludens-1, which are present between ECs and also due to the action of transporters such as p-glycoprotein (P-gp) that efflux molecules that enter the endothelium back into the vessel lumen<sup>1,2,3</sup>. The BBB however allows for the transport of essential molecules such as nutrients (glucose, iron, amino acids) by specific transporters expressed on the EC plasma membranes<sup>1,2,3</sup>. The EC layer is highly polarized with respect to the distribution of the various transporters between the luminal (blood-facing) and abluminal (brain-facing membranes) to allow for the specific and vectorial transport function<sup>4,5</sup>. While the BBB is protective with respect to tightly regulating the CNS milieu, it is a major challenge for CNS drug delivery in diseases such as Parkinson's with a functional BBB. Even in neurological diseases with BBB dysfunction, it cannot be assumed that the brain drug delivery is increased particularly as the barrier dysfunction could include damage to the specific transporter targets for example as in Alzheimer's disease (AD). In AD, several amyloid beta transporters such as LRP1, RAGE, P-gp are known to be dysregulated and hence targeting these transporters might be futile<sup>6,7,8</sup>. The BBB is impaired in several neurological diseases such as stroke, AD, meningitis, multiple-sclerosis, and in brain tumors<sup>9,10,11</sup>. Restoring the barrier function is a crucial part of the therapeutic strategy and thus its assessment is critical.

In this work, we have described an objective and quantitative protocol for permeability assay in rodents that we successfully applied to several mouse lines both transgenic and experimental disease models<sup>10,12,13,14</sup>. The method is based on a simple intraperitoneal injection of fluorescent tracers followed by perfusion of the mice to remove the tracers from the vascular compartment. Brain and other organs are collected post perfusion and permeability assessed by an objective and absolute permeability index based on fluorescence measurements of tissue homogenates in a plate reader. All raw fluorescence values are corrected for the background using tissue homogenates or serum from sham animals that do not receive any tracer. Ample normalizations are included for serum volume, serum fluorescence, and the weight of the tissues,

thus yielding permeability index that is absolute and comparable between experiments and tissue types. For ease of comparison between groups, the absolute permeability index values can be readily transformed to ratios as we had performed previously<sup>12</sup>. Concurrently, stored hemi-brains and kidney could be utilized for tracer visualization by fluorescence microscopy<sup>10</sup>. The classic fluorescence microscopy could be valuable in obtaining regional difference in permeability albeit cumbersome due to subjective selection of tissue sections and images for a semi-quantitative analysis. The detailed steps are presented in the protocol and notes are added where appropriate. This provides the necessary information for successfully performing the *in vivo* permeability assay in mice that can be scaled to other small animals. The assay can be applied to many kinds of tracers allowing for the charge and the size based permeability assessment by a combination of tracers with distinct fluorescence spectra.

## Protocol

All animals were handled with utmost care minimizing pain or discomfort during the procedure. This procedure follows the animal care guidelines of our institution and has been approved by the local committee (Regierungspraesidium Darmstadt, approval number FK/1044).

A schematic of the work steps for *in vivo* permeability assay in mice is shown in **Figure 1**. The details of each step are described below.

## 1. Animal Handling

### 1. Preparation and administration of tracers and anesthetics

1. Prepare labeled tubes and molds for tissue embedding at least a day before the permeability assay. Maintain sterile conditions throughout the protocol by working under clean fume hood and using tools cleaned with 80 % ethanol. Use male or female wild-type (WT) or angiotensin-2 (Ang-2) gain-of-function (GOF) CD1 mice in the mature adult age group of 3-6 months for the current protocol. Perform genotyping of the mice as described previously<sup>10</sup>.  
Note: 80% alcohol will not result in sterile instruments but will minimize contamination of the samples prepared.
2. Dilute all the tracers in sterile PBS into 2 mM stocks and store the aliquots protected from light at -20 °C.
3. Choose tracers such as (Tetramethyl Rhodamine) TMR and (fluorescein isothiocyanate) FITC with distinct excitation/emission spectra and that are lysine fixable resulting in minimal interference between the dyes both by fluorescence microscopy (using the TMR or FITC filter respectively) and by fluorometry in a plate reader for the permeability assay.  
NOTE: TMR dextran 3 kD and FITC dextran 3 kD used in the study are both lysine fixable and hence could be also used for immunohistochemical analysis post-fixation with aldehydes in order to investigate regional differences.
4. Handle all animals with utmost care following the institutional care guidelines. Inject intraperitoneally each mouse with 100 µL tracer solution that can be increased up to 200 µL when an additional tracer is combined using 100 µL of each tracer in a 1:1 mix<sup>10,13</sup>. Inject at least one animal with PBS alone instead of the tracers to serve as sham control for autofluorescence background subtraction.
5. 5 min after tracer injection, anesthetize the animal with an i.p injection of Ketamine and Xylazine (100 mg and 5-10 mg in 0.9 % Saline per kg body weight respectively, 150 µL of the cocktail per 25 g mouse).  
NOTE: Vet ointment was not applied on eyes during the procedure as the period between animal anesthesia and perfusion/sacrifice was brief (10 minutes) where any drying of the eyes was not observed.

### 2. Blood collection and cardiac perfusion

1. Prepare the animals for cardiac perfusion 10 min after anesthetic administration. Check the absence of paw twitch response in order to ensure that the animal reached a surgical plane of anesthesia.
2. Lay the animals on their back and apply 80 % ethanol on the skin of abdominal area. Using small scissors, open up the abdominal wall with a small incision (2 cm) just beneath the rib cage. Separate liver from the diaphragm and then slowly cut through the diaphragm exposing the pleural cavity<sup>15</sup>.
3. Cut the rib cage bilaterally and fix the cut sternum in order to expose the left ventricle. Insert a 21-gauge butterfly needle connected to a peristaltic perfusion system in the posterior of the left ventricle.
4. Puncture the right atrium and quickly (within 10 s) collect 200-300 µL of blood released into the chest cavity using 1 mL pipette tips (with end cut-off) in serum collection tubes and store it on ice.  
Note: This perfusion procedure is non-survival.
5. As soon as the blood is collected, switch on the perfusion system (10-12 rpm, 5 mL/min) and perfuse the animal for 3 min with warm (RT) 1x PBS (free of Ca<sup>2+</sup>/Mg<sup>2+</sup> ions).  
NOTE: PBS containing Ca<sup>2+</sup>/Mg<sup>2+</sup> ions can be utilized for better heart activity during the perfusion. The total amount of PBS used for perfusion is in the range of 15-20 mL.
6. Assess perfusion quality by noting the color of liver, kidneys, which appear white/pale after perfusion.  
NOTE: Kidney or liver perfusion do not necessarily indicate brain perfusion as the arteries (carotid/vertebral) reaching the brain from aorta might get ruptured during the preparation in step 3 particularly during the atrial puncture.

## 2. Tissue Processing

### 1. Organ collection and storage

1. At the end of the perfusion, confirm death of the animal by cervical dislocation and harvest brain and kidneys. Verify brain perfusion by the color of the brains (no visible blood in vessels of the meninges), so as to exclude the animals from permeability analysis when perfusion quality is not good. Separate the brain into 2 hemibrains using a scalpel (**Figure 1**).
2. Dissect with a scalpel one hemisphere free of olfactory lobes and cerebellum and transfer the hemisphere to a 2-mL tube. Store hemisphere in an additional tube if required for cerebellar permeability assessment.
3. Transfer a single kidney to another 2-mL tube. Store the samples immediately on dry ice.

4. Embed natively the remaining kidney and hemi-brain (comprising the cerebellum and olfactory lobes) in tissue-tek optimal cutting temperature (O.C.T) compound on dry ice.
5. In the end, centrifuge the blood samples stored on ice in serum collection tubes at 10,000 g, 10 min at 4 °C. Transfer serum supernatants to 1.5 mL tubes and place them in the dry ice container.
6. Transfer all the samples collected on dry-ice to -80 °C freezer until further processing.  
NOTE: It is important to freeze the samples before proceeding to the homogenization steps as homogenization efficiency increases after as freeze thawing.

## 2. Homogenization and centrifugation

1. Thaw on ice the hemi-cerebrum and kidney samples frozen down at -80 °C and weigh the tubes containing the organs. From these weights, subtract the mean value of several empty tubes (about 20) to get the tissue weight. Add 300 µL and 200 µL of cold 1X PBS to the tubes containing kidney and hemi-cerebrum, respectively.  
NOTE: For lower amounts of tissue (like hemi-cerebellum, below 100 mg) weighing the individual tubes is recommended.
2. Homogenize each sample in the original eppendorf tube with a polytetrafluoroethylene (PTFE) pestle attached to an electric overhead stirrer (1,000 rpm) by performing about 15 strokes (1 stroke = 1 up and 1 down). Rinse the pestle with PBS in between samples and wipe dry before proceeding to the next sample.  
NOTE: The use of detergents during homogenization was avoided due to potential interference with fluorometry. However, intracellular tracer is also detected in this protocol as the tissue is thoroughly homogenized, which is more efficient after one round of freeze thawing.
3. Store the homogenized samples on ice protected from light and centrifuge all together in the end at 15,000 g, 20 min, 4 °C in a tabletop centrifuge. Transfer supernatants to a new 1.5 mL tubes on ice for immediate fluorometry or at -80 °C to be analyzed later.

## 3. Fluorescence measurement and quantification

1. If frozen at the end of the previous step, thaw on ice the tissue supernatant and serum samples stored at -80 °C protecting them from light with the foil.
2. Pipette 50 µL of diluted serum (30 µL 1x PBS + 20 µL serum) or tissue supernatants (as is) into a 384-well black plate. Include at least one sample from sham animal for serum and tissue supernatants to ensure proper background subtraction, as this tissue homogenate background is normally higher than that of PBS used as the diluent.  
NOTE: An average of 3 sham animals can be used for autofluorescence although a very little variability in sham autofluorescence values (data not shown) was observed. The amount of serum used can be reduced by diluting it with PBS, which can also increase the signal to noise ratio for samples with low fluorescence such as the brain samples. Up to 10 µL serum was tested diluting it with 40 µL PBS. Make sure that no bubbles are present in the wells.
3. Insert the 384-well black plate into the plate reader and open a new script selecting fluorescence measurement.
4. Set the gain to optimal and use excitation/emission (nm) values of 550/580 or 490/520 for TMR or FITC dye respectively and start the measurement to obtain the raw fluorescence units (RFUs).
5. Use the raw fluorescence units (RFUs) from the plate reader to calculate the permeability index (PI) after subtracting the corresponding sham values.
  1.  $\text{*Permeability Index (mL/g)} = (\text{Tissue RFUs/g tissue weight}) / (\text{Serum RFUs/mL serum})$
6. Example calculation for brain permeability index (PI) of the animal GOF1 (Table 1):
  1. GOF1 brain RFUs - SHAM brain RFUs = 154 - 22.5 = 131.5
  2. GOF1 serum RFUs - SHAM serum RFUs = 38305 - 27 = 38278
  3. Brain weight (g) = 0.195
  4. Serum volume (ml) = 0.02
  5. Brain Permeability Index ( $10^{-3}$  mL/g) =  $(131.5/0.195)/(38278/0.02) = 0.352$   
NOTE: The permeability index calculations yield values that are absolute and comparable between experiments and tissue types. These however can be presented as ratios for ease of comparison between 2 groups<sup>12</sup>. This can be achieved by dividing the PI of each animal in both groups with the mean PI of control group, driving the control group mean through 1 yet keeping the inter animal variation in the control group. This transformation provides values for experimental group (or groups) relative to control group set to 1.

## 4. Immunofluorescence visualization of tracer

1. Cut the kidney/hemi-brain blocks embedded natively in tissue-tek compound (O.C.T) (step 2.1) into 10 µm sections on a cryostat set to -20 °C and transfer the sections to slides placed at room temperature. Once the sections are dried (about 30 min), transfer slides to -80 °C freezer until use.
2. On the day of staining, thaw the slides at 37 °C for 10 min, and then fix the sections with 4% paraformaldehyde (PFA) for 10 min at room temperature followed by quick washing in PBS.
3. Incubate the sections in permeabilization/blocking buffer made of sterile PBS containing 1 % BSA and 0.5 % Triton X-100 pH 7.5 for 1 h at room temperature.
4. Incubate slides for 1.5 h at room temperature with CD31 primary antibody (0.5 mg/ml, clone MEC 13.3), diluted in 1:100 in buffer containing sterile PBS, 0.5 % BSA, 0.25 % Triton X-100 (pH 7.2) followed by three 5 min washes in PBS.
5. Perform secondary antibody incubation in the above buffer for 1 h at room temperature with species-specific fluorescently labeled antibodies diluted 1:500 (2 mg/mL). For CD31, goat anti-rat Alexa 568 or Alexa 488 can be used at a dilution of 1:500. Include DAPI (300 µM) in the secondary antibody mix (1:1,000 dilution from the stock) to stain for the nuclei.
6. Mount the stained sections with aqua polymount and leave it overnight for polymerization at room temperature in dark.
7. Acquire images using a spectral imaging confocal laser scanning microscope system. Analyze images by NIS elements software (version 4.3). Software such as Photoshop can be used for generation of montage figures.

## Representative Results

We have recently shown that angiotensin-2 (Ang-2) gain-of-function (GOF) mice have higher brain vascular permeability than control mice in healthy conditions<sup>10</sup>. In stroke-induced mice, it was also shown that the GOF mice had bigger infarct sizes and greater permeability than the control littermates. These results show a critical role of Ang-2 in permeability at the BBB. The protocol therefore utilized the GOF mice and compared them to control littermates to describe the *in vivo* permeability assay. However, this method can be applied to any disease model, transgenic mouse model or drug treatments that alter the BBB permeability as we did previously<sup>10,11,12,13</sup>.

A short circulation time (15 min) for permeability analysis is suggested, as longer circulation times will lead to a greater clearance from the vascular compartment, which has been observed also in previous studies<sup>16</sup>. The clearance of 3 kD FITC-dextran at 2 h (**Figure 2 C, D**) is much greater than at 15 min (**Figure 2 A, B**) in kidney as well as in brain tissue. In the brain, there is very little extravascular tracer due to intact blood-brain barrier in these adult WT mice (**Figure B, D**). Applying this method, the tracer permeability in Ang-2 GOF with WT littermates was compared. The results presented in a table format (**Table 1**) indicate higher tracer accumulation in the brains of GOF mice compared to WT mice. However, the kidney fluorescence is not altered between these groups. Immunofluorescence images confirm the increase in extravascular tracer in GOF mice (**Figure 3 B, D**) when compared to WT mice (**Figure 3 A, C**) where the tracer is limited to vascular compartment.

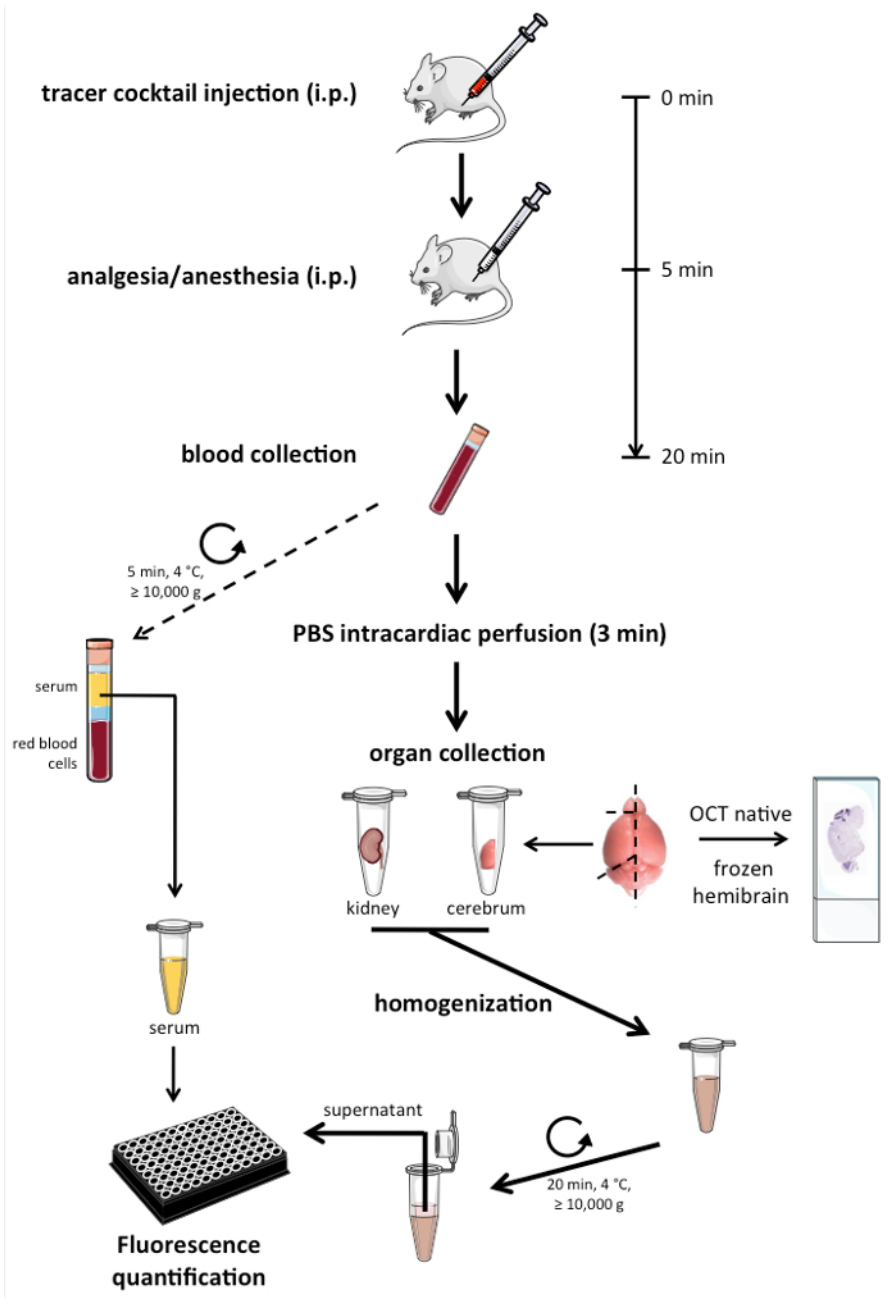


**Figure 1.** Schematic of the workflow for the *in vivo* permeability assay using fluorescent tracers. [Please click here to view a larger version of this figure.](#)

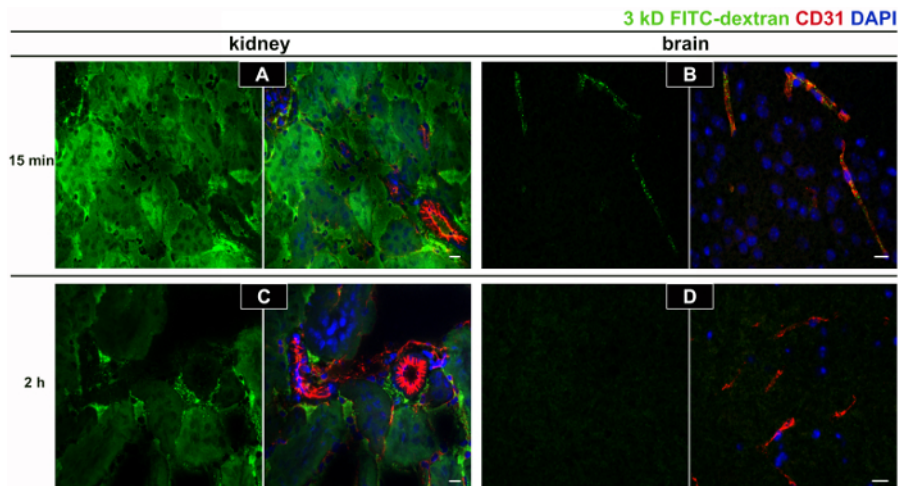


**Figure 2. Tracer clearance at short and long circulation times.** In order to establish the tracer circulation time for the permeability assay, a short circulation time of 15 min (A, B) was compared to a long circulation time of 2 h (C, D) post tracer injection. The longer circulation time of 2 h led to very low amounts of tracer accumulation in kidney (C) where the basal permeability is high compared to a short 15 min circulation time (A) potentially due to a very high clearance of FITC dextran-3 kD (green channel) from the vascular compartment. This effect was even more dramatic in the brain characterized by the tight blood-brain barrier (B, D). CD31 staining (red channel) confirmed the presence of vessels in the region of interest. Representative images from a single animal out of 2 wild-type adult CD1 mice injected with the tracer for each time point and animals were sacrificed without perfusing them to visualize the intravascular tracer. The scale bar = 20 μm. [Please click here to view a larger version of this figure.](#)

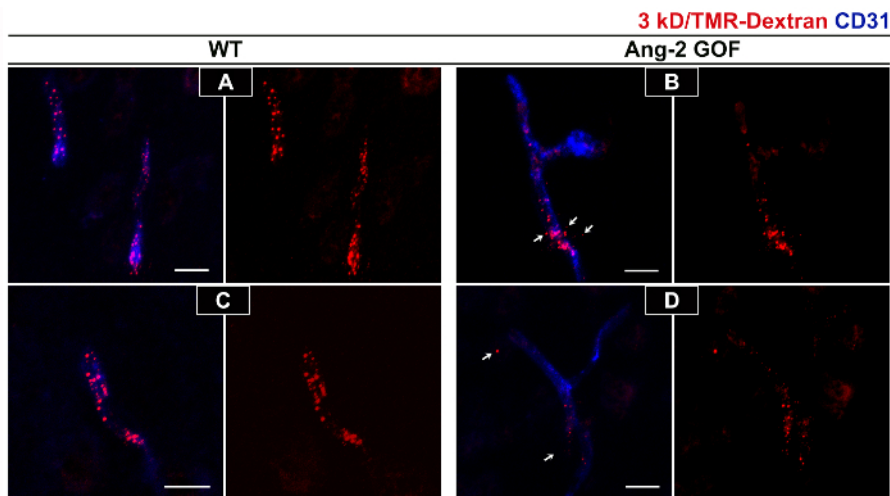


**Figure 3. Immunofluorescence staining for tracers to assess brain permeability changes in GOF mice.** Increased permeability of 3 kD TMR-dextran tracer (in red) can be visualized in Ang-2 GOF mice (B, D) compared to WT littermates (A, C) in the cortex region. In WT animals the tracer is restricted to the vessels (A, C) whereas extravascular tracer can be observed in GOF mice (white arrows in B, D). Staining for CD31 (in blue) in the merged images (A-D) confirms the presence of vessels. Figure shows representative images from 2 WT and 2 GOF mice injected with tracers i.p and sacrificed 15 min post injection with perfusion. Scale bar = 20 μm. [Please click here to view a larger version of this figure.](#)

Animal ID	Brain Weight (g)	Kidney Weight (g)	Serum volume (mL)	Serum RFU	Kidney RFU	Brain RFU	Perm. Index (10 <sup>-3</sup> ml/g)	
							Kidney	Brain
GOF 1	0.195	0.252	0.02	38305	31051	154	64.4	0.352
GOF 2	0.177	0.249	0.02	42001	31411	126	60	0.278
WT 1	0.167	0.301	0.02	40904	31591	64	51.2	0.122
WT 2	0.146	0.294	0.02	39502	31768	70	54.8	0.164
SHAM	0.155	0.27	0.02	27	36	22.5	NA	NA

**Table 1. Tissue permeability calculations.** Permeability index calculations for Ang-2 gain-of-function (GOF) and wild-type littermates (WT) mice clearly show greater (about 2-fold) brain permeability in GOF mice compared to WT mice. The kidney permeability is however in the same range between the 2 groups. The basal kidney permeability is much greater compared to brain as expected due to fenestrated endothelium in kidney that do not form a tight barrier.

## Discussion

Blood-brain barrier dysfunction is associated with a number of neurological disorders, including primary and secondary brain tumors or stroke. BBB breakdown is often associated with life-threatening CNS edema. The elucidation of the molecular mechanisms that trigger the opening or closure of the BBB is therefore of therapeutic significance in neurological disorders and commonly investigated by researchers. However, methods to investigate BBB permeability *in vivo* reported in the literature, are often associated with technical difficulties that depend on tedious and subjective quantification of fluorescence images<sup>17,18,19</sup>. Furthermore, some of the methods include whole brain fluorescence imaging that is fallacious as it more indicative of permeability of superficial brain vessels that do not form a tight barrier. Even when quantification has been performed based on the objective brain tissue absorbance (e.g. Evans blue permeability assessment) the animals are often not perfused leading to erroneous interpretation due to significant blood fraction. Brain weight is another variable that is often not included in permeability calculations but needs to be as edema resulting from vascular permeability can increase the weight and alter the net permeability. Furthermore, sex and animal-to-animal brain weight variations can cloud permeability differences. Radioactive tracers such as <sup>14</sup>C sucrose and [3H] inulin have been successfully applied for brain permeability index but do not offer the wide range of size and charge based permeability investigation as with fluorescently labeled tracers<sup>20</sup>.

For the above reasons, we adopted a method that is simple, objective and quantitative in estimating blood-brain barrier permeability *in vivo* in mice using fluorescently labeled tracers. Dextran is a hydrophilic polysaccharide characterized by its moderate-to-high molecular weight (3-200 kD) and can be obtained as charged or uncharged molecules based on the conjugated fluorophore. Endothelial tight junctions formed by mainly claudins (1, 3, 5 and 12) and occludin, together determine the paracellular size and charge selectivity by the charge pore residues present on their first extracellular loop (reviewed in<sup>21</sup>). Permeability across blood-brain barrier *in vivo* is also dependent upon glycocalyx and the basal lamina, two structures that are present on either side of the BBB<sup>22,23</sup>. Luminally present glycocalyx is a gel like structure formed by negatively charged oligosaccharides (heparin sulfates) that also acts as a barrier to blood-borne macromolecules such as albumin. Changes in the glycocalyx thickness or composition are also associated with vascular permeability changes as we observed in angiotensin-2 gain of function mice compared to wild type mice<sup>10</sup>. The basement membrane on the other hand is present on the abluminal side of the endothelial cells comprising both the vascular basement membrane made by endothelial cells and pericytes whereas the parenchymal basement membrane or astrocytic basement membrane made by astrocytes. These basement membranes are also negatively charged and thus also have capacity to serve as charge barriers. In this regard, conjugated dextrans offer investigation of both size and charge-based permeability. For example, TMR-dextran 3 kD is anionic whereas TXR-dextran 3 kD is neutral, combining one of these tracers with a conjugated high molecular weight dextran such as FITC dextran 70 kD in the same mix injected to the mice, one could assess the size-based permeability. We further take advantage of the lysine-fixable nature of fluorescent-labeled dextrans to explore the regional differences in permeability in standard immunofluorescence staining. Dextrans also generally exhibit low immunogenicity and thus serve as good tracers. Lucifer yellow, cadaverine, fluorescein-5-thiosemicarbazide (FTSC), are among other tracers that are in the low molecular weight range (0.4-0.8 kD) and are fixable.

In our method, the tracers were injected by i.p route followed by perfusing the mice and obtaining the fluorescence of brain homogenates normalized to the wet weight and the serum fluorescence. This is a simple yet highly quantitative and objective method as there is no selection of sections/images as in quantification by immunofluorescence method that is classically used. We utilize only one hemi-brain for the permeability assay and utilize the other hemibrain for immunofluorescence staining by analyzing sagittal sections providing regional differences in the same animal. The use of each hemi-brain for distinct concurrent measurements is one of the main advantages in our protocol. Also, permeability of other organs such as kidneys, liver, etc. serves as a good internal control as the basal permeability is high in these organs. In order to compare 2 groups, one would have to first subtract the sham animal (that did not receive tracer injection) autofluorescence from all the animals in both groups and all the tissue types (kidney, brain, and serum) for each tracer and then proceed to normalized calculations comparing the 2 groups. The permeability index (PI) is presented that is obtained as a ratio of tissue to serum fluorescence normalized to tissue weight and serum volume. Our calculations yield an absolute value for the tracer permeability that can be compared between experiments and tissue types. These values however, can be easily expressed as ratios or percent between the 2 groups being compared as we have also done previously<sup>12</sup>. This can be achieved by dividing the PI of each animal in both the groups with the mean PI of all animals in the control group. This would drive the control group PI through 1 yet keeping the error between the animals and for the experimental group give values that are relative to the control group mean of 1.

Injection of tracers by i.p is easier, but more cost intensive compared to i.v injection, as the amount of tracer needs to be increased. Our data (not shown) in this regard indicates that nearly 2-fold higher amount in the tracer is required by i.p injection compared to i.v to obtain similar serum fluorescence values. Also, the time of circulation is higher in i.p route compared to i.v due to the time taken for tracer absorption into the blood stream. In this regard, serum fluorescence values at 15 min post i.p injection were comparable to 5 min post i.v injection for tracers in the low and medium molecular weight range between 0.4-4 kD (data not shown). We suggest a short circulation time because paracellular permeability is linear and if considerable tissue fluorescence is detected post perfusion after a short circulation time (15 min), it already indicates a permeability phenotype as we have reported in our previous publications<sup>10,12,13,14</sup>. Yet at the same time one could obtain the serum fluorescence for normalization. At longer circulation times, tissue clearance is considerable, which reduces serum fluorescence considerably and thus might impact permeability values normalized to serum. While the time of circulation in relation to the size/charge of the tracer has to be optimized for each scenario, we suggest a short circulation time as the starting point. This also applies to higher molecular weight solutes such as plasma IgGs and fibrinogen (150-400 kD) whose permeability characteristics are unlike inert dextran tracers due to their extremely large size and specific interaction with cellular receptors such as Fc receptors that change their half-life<sup>24</sup>. Dextrans on the other hand do not have any specific transport system at the endothelial level<sup>25</sup> and as brain endothelial cells do not undergo pinocytosis to significant levels due to very low levels of plasmalemma vesicle associated protein (PLVAP)<sup>26</sup>, the main route of transport of dextrans is paracellular. We have applied the above method successfully in several scenarios such as permeability in transgenic mice compared to wild-type littermates and also assessed permeability changes in wild type mice after therapeutic intervention<sup>10,12,13,14</sup>. In summary, combined with the immunofluorescence staining, the permeability assay described here is a simple and a robust method to assess the permeability of mice *in vivo* that can be also applied to other small animals.

## Disclosures

The authors declare that they have no competing financial interests.

## Acknowledgements

The authors would like to acknowledge Sphingonet consortium funded by the Leduq foundation for supporting this work. This work was also supported by the Collaborative Research Center "Vascular differentiation and remodeling" (CRC/ Transregio23, Project C1) and by the 7. FP, COFUND, Goethe International Postdoc Programme GO-IN, No. 291776 funding. We further acknowledge Kathleen Sommer for her technical assistance with mice handling and genotyping.

## References

- Abbott, N. J., Rönnbäck, L., & Hansson, E. Astrocyte-endothelial interactions at the blood-brain barrier. *Nature reviews. Neuroscience*. **7** (1), 41-53 (2006).
- Zhao, Z., Nelson, A. R., Betsholtz, C., & Zlokovic, B. V. Establishment and Dysfunction of the Blood-Brain Barrier. *Cell*. **163** (5), 1064-1078 (2015).
- Obermeier, B., Daneman, R., & Ransohoff, R. M. Development, maintenance and disruption of the blood-brain barrier. *Nature Medicine*. **19** (12), 1584-1596 (2013).
- Devraj, K., Klinger, M. E., Myers, R. L., Mokashi, A., Hawkins, R. A., & Simpson, I. A. GLUT-1 glucose transporters in the blood-brain barrier: differential phosphorylation. *Journal of neuroscience research*. **89** (12), 1913-1925 (2011).
- Banks, W. A. From blood-brain barrier to blood-brain interface: new opportunities for CNS drug delivery. *Nature reviews. Drug discovery*. **15** (4), 275-292 (2016).
- Zlokovic, B. V. Neurovascular pathways to neurodegeneration in Alzheimer's disease and other disorders. *Nature reviews. Neuroscience*. **12** (12), 723-738 (2011).
- Paganetti, P., Antonello, K., et al. Increased efflux of amyloid- $\beta$  peptides through the blood-brain barrier by muscarinic acetylcholine receptor inhibition reduces pathological phenotypes in mouse models of brain amyloidosis. *Journal of Alzheimer's disease: JAD*. **38** (4), 767-786 (2014).
- Devraj, K., Poznanovic, S., et al. BACE-1 is expressed in the blood-brain barrier endothelium and is upregulated in a murine model of Alzheimer's disease. *Journal of cerebral blood flow and metabolism: official journal of the International Society of Cerebral Blood Flow and Metabolism*. **36** (7), 1281-1294 (2016).
- Daneman, R. The blood-brain barrier in health and disease. *Annals of neurology*. **72** (5), 648-672 (2012).
- Gurnik, S., Devraj, K., et al. Angiotensin-2-induced blood-brain barrier compromise and increased stroke size are rescued by VE-PTP-dependent restoration of Tie2 signaling. *Acta neuropathologica*. **131** (5), 753-773 (2016).
- Scholz, A., Harter, P. N., et al. Endothelial cell-derived angiotensin-2 is a therapeutic target in treatment-naive and bevacizumab-resistant glioblastoma. *EMBO Molecular Medicine*. **8** (1), 39-57 (2016).
- Gross, S., Devraj, K., Feng, Y., Macas, J., Liebner, S., & Wieland, T. Nucleoside diphosphate kinase B regulates angiogenic responses in the endothelium via caveolae formation and c-Src-mediated caveolin-1 phosphorylation. *Journal of cerebral blood flow and metabolism: official journal of the International Society of Cerebral Blood Flow and Metabolism*. **37** (7), 2471-2484 (2017).
- Ziegler, N., Awwad, K., et al.  $\beta$ -Catenin Is Required for Endothelial Cyp1b1 Regulation Influencing Metabolic Barrier Function. *The Journal of neuroscience: the official journal of the Society for Neuroscience*. **36** (34), 8921-8935 (2016).
- Vutukuri, R., Brunkhorst, R., et al. Alteration of sphingolipid metabolism as a putative mechanism underlying LPS-induced BBB disruption. *Journal of Neurochemistry*. (2017).
- Gage, G. J., Kipke, D. R., & Shain, W. Whole Animal Perfusion Fixation for Rodents. *J Vis Exp*. (65), e3564 (2012).
- Hoffmann, A., Bredno, J., Wendland, M., Derugin, N., Ohara, P., & Wintermark, M. High and Low Molecular Weight Fluorescein Isothiocyanate (FITC)-Dextrans to Assess Blood-Brain Barrier Disruption: Technical Considerations. *Translational stroke research*. **2** (1), 106-111 (2011).
- Armulik, A., Genov $\acute{e}$ , G., et al. Pericytes regulate the blood-brain barrier. *Nature*. **468** (7323), 557-561 (2010).
- Daneman, R., Zhou, L., Kebede, A. A., & Barres, B. A. Pericytes are required for blood-brain barrier integrity during embryogenesis. *Nature*. **468** (7323), 562-566 (2010).
- Bell, R. D., Winkler, E. A., et al. Pericytes control key neurovascular functions and neuronal phenotype in the adult brain and during brain aging. *Neuron*. **68** (3), 409-427 (2010).
- Banks, W. A., Gray, A. M., et al. Lipopolysaccharide-induced blood-brain barrier disruption: roles of cyclooxygenase, oxidative stress, neuroinflammation, and elements of the neurovascular unit. *Journal of Neuroinflammation*. **12**, 223 (2015).
- Krause, G., Winkler, L., Mueller, S. L., Haseloff, R. F., Piontek, J., & Blasig, I. E. Structure and function of claudins. *Biochimica et biophysica acta*. **1778** (3), 631-645 (2008).
- Johansson, B. B. Blood-Brain Barrier: Role of Brain Endothelial Surface Charge and Glycocalyx. *Ischemic Blood Flow in the Brain*. 33-38 (2001).
- Fu, B. M., Li, G., & Yuan, W. Charge effects of the blood-brain barrier on the transport of charged molecules. *The FASEB Journal*. **22** (1 Supplement), 734.1-734.1 (2008).
- Goebel, N. A., Babbey, C. M., Datta-Mannan, A., Witcher, D. R., Wroblewski, V. J., & Dunn, K. W. Neonatal Fc receptor mediates internalization of Fc in transfected human endothelial cells. *Molecular biology of the cell*. **19** (12), 5490-5505 (2008).
- Lopez-Quintero, S. V., Ji, X.-Y., Antonetti, D. A., & Tarbell, J. M. A three-pore model describes transport properties of bovine retinal endothelial cells in normal and elevated glucose. *Investigative ophthalmology & visual science*. **52** (2), 1171-1180 (2011).



26. Hallmann, R., Mayer, D. N., Berg, E. L., Broermann, R., & Butcher, E. C. Novel mouse endothelial cell surface marker is suppressed during differentiation of the blood brain barrier. *Developmental dynamics: an official publication of the American Association of Anatomists*. **202** (4), 325-332 (1995).